



8th Manufacturing Engineering Society International Conference

Influence of infill and nozzle diameter on porosity of FDM printed parts with rectilinear grid pattern

Irene Buj-Corral^{a,*}, Ali Bagheri^a, Alejandro Domínguez-Fernández^a, Ramón Casado-López^a

^a*Universitat Politècnica de Catalunya. Departament of Mechanical Engineering. School of Engineering of Barcelona (ETSEIB). Av. Diagonal, 647. 08028, Barcelona, Spàin*

Abstract

The aim of the paper is to analyze the effect of nozzle diameter and infill on porosity and pore size of FDM printed specimens with rectilinear grid pattern. Two different nozzle diameters (0.2 and 0.4 mm), as well as four different infill values (20 %, 40 %, 60 % and 80 %) were used. Experimental results for pore size agree with theoretical results. On the contrary, low experimental porosity was obtained, especially for high infill values, because printed samples show fewer pores than expected. The higher infill, the lower porosity and pore size. Higher nozzle diameter implies higher pore size but similar porosity.

© 2019 The Authors. Published by Elsevier B.V.

This is an open access article under the CC BY-NC-ND license (<http://creativecommons.org/licenses/by-nc-nd/4.0/>)

Peer-review under responsibility of the scientific committee of the 8th Manufacturing Engineering Society International Conference

Keywords: Type your keywords here, separated by semicolons ;

1. Introduction

In the Fused Deposition Modelling (FDM) process, a plastic filament is extruded in thin strands and then deposited layer-by-layer. The FDM technology has many advantages: easiness of use, the possibility to employ different kinds of plastic materials, and the fact that it is more cost-effective than other additive manufacturing technologies.

* Corresponding author. Tel.: +34-93-4054015; fax: +34-93-4016693.

E-mail address: irene.buj@upc.edu

Nevertheless, the technique also has drawbacks. For example, printing supports are required in order to print inclined walls, and poorer surface finish is obtained with FDM than with other printing techniques [1,2].

FDM is widely used for the development of new designs in the automotive industry [3] or to manufacture space instrumentation [4]. In addition, FDM parts have many different medical uses, such as customized implants or models for surgical preparation [5].

In order to save printing time and material, printed parts are usually not solid but have a printing pattern or infill that gives them a certain porosity degree [6]. On the other hand, porosity is a key factor when considering the capacity of the printed scaffolds that simulate tissues to assure cell growth, permeability and mechanical strength [7,8]. Different authors have obtained models for the geometry of FDM printed scaffolds. For example, Ahn et al. defined the different layers as elliptical curves which overlap in the vertical direction [9]. Ding et al. overlapped different surfaces representing beads for modeling the geometry of printed parts [10]. In a previous paper by the authors of the present work, porosity of structures with rectilinear infill was modeled as a function of infill, for different nozzle diameters [11]. Theoretically, porosity is calculated as $1 - \text{infill}$ and, thus, for a certain nozzle diameter the higher infill, the lower porosity and pore size. On the contrary, higher nozzle diameter implies a higher distance between filaments and thus higher pore size, in order to achieve a certain infill value [12].

When printing a porous structure it is difficult to select printing parameters that will allow obtaining required porosity and pore size values. This is because most variables of the process are related to the machine operation rather than to the final shape of the final part. In addition, actual porosity and pore size values may differ from theoretical values. In the present paper, pore size and porosity of structures with rectilinear infill pattern are measured as a function of two printing parameters: nozzle diameter and infill. For doing this, different specimens were printed with prismatic shape in polylactic acid (PLA) material, for different infill and nozzle diameter values. Porosity and pore size were determined in three ways: theoretically from the drawing of the parts, from the simulation of a previously presented geometric model [11] and experimentally by means of X-ray tomography. The main objective of the present paper is to study the effect of infill and nozzle diameter on pore size and porosity of FDM printed parts with rectilinear pattern. Experimental pore size and porosity values are compared to theoretical and simulated ones. Results will help to select proper printing parameters to obtain required pore size and porosity values.

Nomenclature

FDM	Fused Deposition Modelling
PLA	Polylactic Acid

2. Methodology

2.1. Printing tests

Prismatic samples of 10 x 10 x 20 mm were printed in a double head Sigma extruder from BCN3D. The shape of the different structures was drawn with Solid Works, taking into account the deformation of the printed filament [12]. The stl files and gcodes were then obtained with Simplify3D software. The rectilinear infill pattern was chosen.

Polylactic acid (PLA) filament in white color was used for printing the specimens. Nozzle diameters of 0.2 and 0.4 mm, and infill values of 20 %, 40 %, 60 % and 80 % were taken into account. Layer height was 0.15 mm for nozzle diameter 0.2 mm and 0.2 mm for nozzle diameter 0.4 mm. Printing speed was 60 mm/s in all cases. Extrusion multiplier was 100 % and printing temperature was 205 °C.

Figure 1 shows an example of printed parts with nozzle diameter 0.4 mm, with infill values 20 % and 40 % respectively.

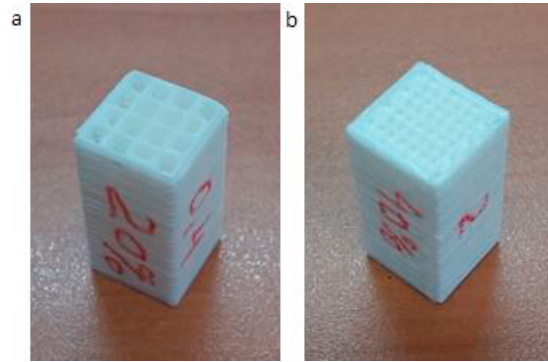


Fig. 1. Printed part with nozzle diameter 0.4 mm and a) 20 % infill, b) 40 % infill.

The printed part with 20 % infill has a regular shape with 16 prismatic channels of square cross-section. On the contrary, the printed part with 40 % infill, with 64 prismatic channels, shows a more irregular shape, with variable wall thickness and with some sealed channels.

2.2. Theoretical determination of pore size and porosity

In order to determine the theoretical pore size and porosity of the specimens, Solid Works software was used to draw the geometry of all samples. With help of Rhinoceros software the volumes of the geometries were verified and double checked. Different printing parameters were taken into account: infill, nozzle diameter and layer height.

In order to obtain the drawings, according to the recommendation of the automatic settings of the Simplify3D software, it was assumed that the total width w (in mm) of the deposited filament is related to nozzle diameter d (in mm), as stated in Equation 1.

$$w = 1.2 \cdot d \quad (1)$$

As an example of the drawn geometries, Figure 2 shows a cross-section of the drawing of the specimens obtained with nozzle diameter 0.4 mm, for 20 % infill and 40 % infill respectively. Orange lines correspond to the plastic material.

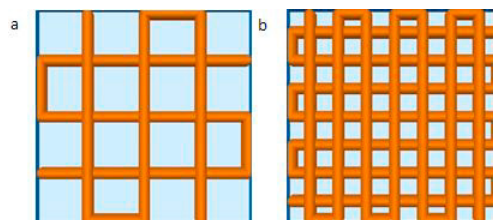


Fig. 2. Cross-section of the drawing of a printed part with nozzle diameter 0.4 mm and: a) 20 % infill, b) 40 % infill.

In Figure 2 it is observed that the specimen with 20 % infill has 16 channels, while the specimen with 40 % infill requires 64 channels.

Once all 3D images were drawn, the porosity of the different structures was calculated with help of Equation 2.

$$\text{Porosity (\%)} = (\text{Total pore volume} / \text{Total volume}) \cdot 100 \quad (2)$$

Where *Total volume* is the volume of the prismatic shape in mm³, and *Total pore volume* is the volume of voids, in mm³, as calculated with Equation 3.

$$\text{Total pore volume} = (\text{Total volume} - \text{Material volume}) \quad (3)$$

Where *Material volume* is the volume of material of the prismatic shape in mm³.

As for pore size, the pores of the rectilinear structure have square cross-section. The distance between contiguous walls was taken into account as the pore size in mm.

Porosity and pore size values are presented in section 3.

2.3. Determination of pore size and porosity by means of simulation

A geometrical model for the rectilinear structure, which was presented in a previous paper, was used to determine simulated values of pore size and porosity. According to the model, porosity is directly related to infill with Equation 4, regardless of nozzle diameter used.

$$\text{Porosity (\%)} = 100 - \text{Infill(\%)} \quad (4)$$

The geometry of the deposited filament is shown in Figure 3, according to the Slic3r manual [12], where *h* is the layer height (mm) and *w* is the filament width (mm).

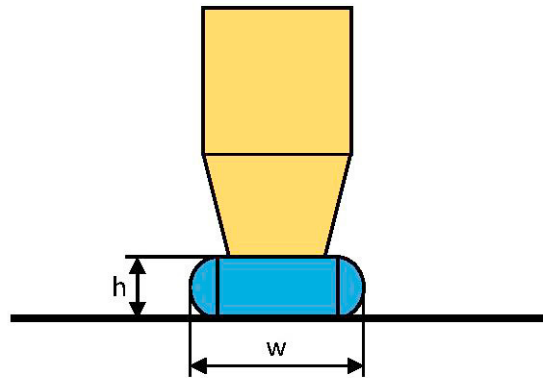


Fig. 3. Geometry of the deposited filaments [11]

The area of the printed filament is obtained from the area of a rectangle and a circle, as stated in Equation 5.

$$\text{Area of printed filament (mm}^2\text{)} = (w - h) \cdot h + \pi \cdot \left(\frac{h}{2}\right)^2 \quad (5)$$

Unless a specific width *w* value is selected, the software takes into account that the area of the printed filament (Eq. 5) is equal to area of the unprinted filament (Eq. 6), where *d* is filament diameter in mm.

$$\text{Area of unprinted filament} = \pi \left(\frac{d}{2}\right)^2 \quad (6)$$

Equating both expressions, Equation 7 is derived.

$$\pi\left(\frac{d}{2}\right)^2 = (w-h) \cdot h + \pi \cdot \left(\frac{h}{2}\right)^2 \quad (7)$$

Extrusion width w is calculated as a function of layer height h and filament diameter d (Eq. 8):

$$w = \frac{\pi\left(\frac{d}{2}\right)^2 - \pi \cdot \left(\frac{h}{2}\right)^2}{h} + h = \frac{\pi\left(\frac{d}{2}\right)^2 + (4-\pi) \cdot \left(\frac{h}{2}\right)^2}{h} \quad (8)$$

Figure 4 depicts the distance between trajectories of the nozzle, or distance between parallel filaments.

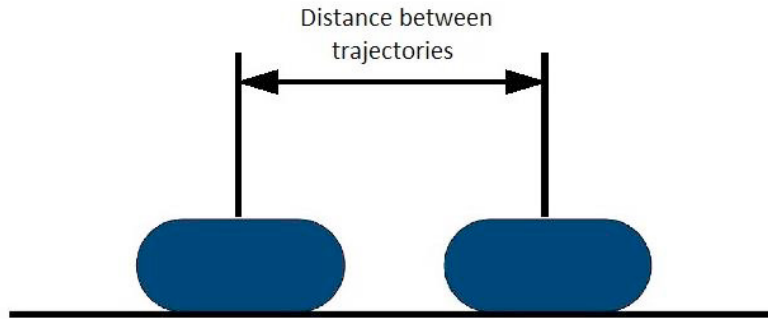


Figure 4. Distance between trajectories for the rectilinear grid pattern [11]

The definition of infill is presented in Eq. 9. Assuming that h^2 is close to zero, from Eq. 5 it can be deduced that Area of printed filament is almost equal to $w \cdot h$. Thus, the volume of the printed parts would correspond to $w \cdot h \cdot l$. The total volume of the part is equal to distance between trajectories of the grid pattern $\cdot h \cdot l$.

$$\text{Infill} = \frac{\text{Volume of printed part}}{\text{Total volume of the part}} = \frac{w \cdot h \cdot l}{\text{Distance between trajectories of the grid pattern} \cdot h \cdot l} \quad (9)$$

Where l is the length of the printed filament in mm.

If terms are joined, equation 10 is obtained.

$$\text{Distance between trajectories of the grid pattern} = \frac{w}{\text{infill}} \quad (10)$$

Pore size is equal to distance between trajectories minus filament width (Eq. 11).

$$\text{Pore size} = \text{Distance between trajectories of the grid pattern} - w \quad (11)$$

Thus, pore size can be written as a function of infill and width, according to Equation 12.

$$\text{Pore size} = \frac{w}{\text{infill}} - w = w \left(\frac{1}{\text{infill}} - 1 \right) = \frac{1}{h} \left(\left(\frac{1}{\text{infill}} - 1 \right) \left(\pi \left(\frac{d}{2} \right)^2 - (4-\pi) \cdot \left(\frac{h}{2} \right)^2 \right) \right) \quad (12)$$

Where w is the width of the deposited filament (mm), d is the initial diameter of the filament corresponding to the nozzle diameter (mm) and h is final height of the deposited filament or layer height (mm).

For printing thermoplastic materials, it is recommended that layer height h ranges between 0.5 and 0.8 times the nozzle diameter d . In the present work, the average value of the interval was considered (Equation 13).

$$h = 0.65 \cdot d \quad (13)$$

From the combination of equations 2 and 3, pore size was calculated as a function of infill, nozzle diameter d and layer height h . Results will be presented in section 3.

2.4. Experimental determination of pore size and porosity

A Zeiss Metrotom 800 X-ray tomography equipment was used for obtaining 3D images of the printed samples. From the images, with help of VG Studio Max software, Total pore volume and porosity were calculated according to Equations 2 and 3 respectively.

For each image, a cross-section was obtained at a height of 10 mm (half the height of the samples), where pore size was measured. Specifically, pore size was considered to be the side of the square voids or the distance between contiguous walls. Four different measurements were taken on each sample, and the average pore size value was calculated for each sample.

Figure 5 shows X-ray tomography cross-sections of two different samples printed with nozzle diameter 0.4 mm, with infill 20 % and 40 % respectively.

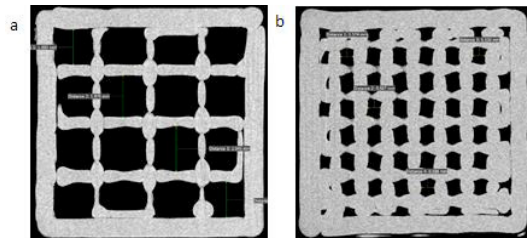


Fig. 5. X-ray tomography of samples with nozzle diameter 0.4 mm and: a) infill 20 %, b) infill 40 %.

Figure 5a, corresponding to infill 20 %, shows a regular structure with 16 square holes. On the contrary, Figure 5b, corresponding to infill 40 %, depicts holes with the shape of irregular parallelograms. In addition, walls have variable thicknesses and not all the 64 theoretical holes are observed.

3. Results

3.1. Pore size

In order to compare pore size values, theoretical, experimental and simulated pore size results are presented vs infill in Figure 6.

Similar results were obtained for theoretical, simulated and experimental pore size values. Pore size decreases with infill for both nozzle diameters studied. When higher nozzle diameter of 0.4 mm is used, thicker walls are printed, and thus walls have to be more separated in order to get a certain infill value. For this reason, higher pores are required for nozzle diameter 0.4 mm than for nozzle diameter 0.2 mm.

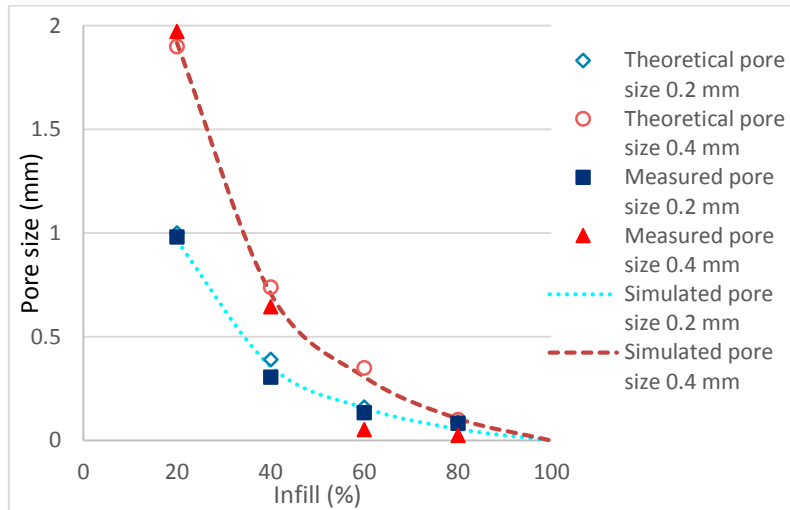


Fig. 6. Pore size (mm) vs. Infill (%)

The shape of the curves was similar to that reported in [11] for ceramic parts.

3.2. Porosity

In order to compare the different values, theoretical, simulated and experimental porosity results are presented vs. infill in Figure 7.

Porosity decreases with infill as expected. Theoretical porosity values are very similar to simulated porosity values. Experimental porosity coincides with theoretical and simulated porosity at infill 20 %. This corresponds to the regular shape observed in Figures 1a and 3a. However, higher infill values, seen in Figures 1b and 3b, lead to more irregular shapes, with some pores that are blocked with plastic material. This suggests that, although the pore size is correct, some pores are missing, due to an excess of material when printing. Thus, measured porosity is lower than expected.

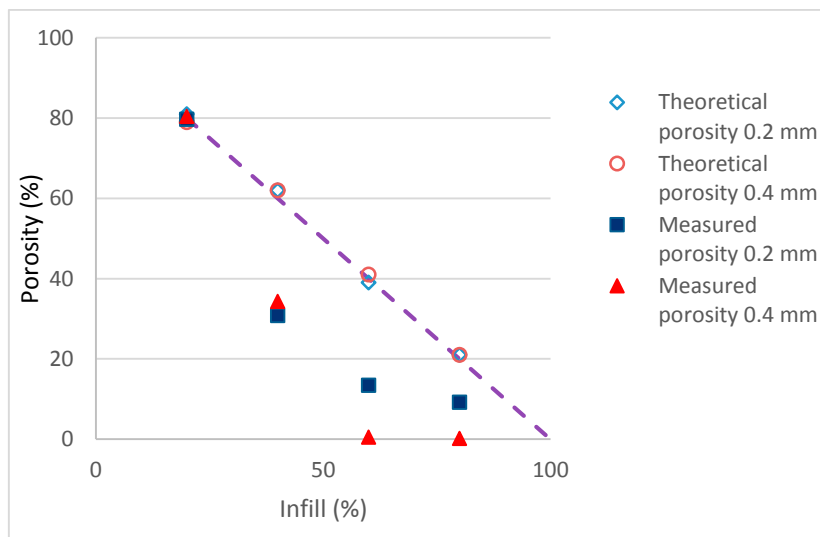


Fig. 7. Porosity (%) vs. Infill (%)

In order to improve the shape of printed parts, in the future the effect of the parameter Extrusion multiplier on porosity can be studied. Extrusion multiplier modifies the quantity of material to be extruded per time unit. In addition, the effect of printing temperature on porosity can be considered.

4. Conclusions

In the present work porosity and pore size results are presented for different nozzle sizes and different infill values in FDM processes. Both porosity and pore size were determined theoretically (from a 3D representation), from the simulation with a geometrical model and experimentally by means of X-ray tomography.

Main conclusions are as follows:

- Samples printed with high infill show more irregular structures than samples printed with low infill. Since the rectilinear grid structure was used as infill pattern, structures consist of square prismatic channels separated by parallel and perpendicular walls. High infill implies variable wall thickness, with channels having irregular shape and with some blocked channels.
- Pore size decreases with infill. Higher pore size is obtained when higher nozzle diameter is used. Similar results were reported for theoretical, simulated and experimental values, for all infill values considered between 20 % and 80 %.
- Porosity decreases with infill as expected, regardless of nozzle diameter used. Similar results were obtained for theoretical and simulated calculations. On the contrary, experimental porosity was lower than expected at infill values of 40 % or higher. This suggests that the amount of material when printing was excessive. Thus, in the future, the extrusion multiplier parameter will be considered.

Acknowledgements

The authors thank the Spanish Ministry of Industry, Economy and Competitiveness for the financial help of project DPI2016-80345R.

References

- [1] H. Lipson, M. Kurman, *Fabricated : The New World of 3D Printing*, n.d.
- [2] I. Gibson, D. Rosen, B. Stucker, *Additive Manufacturing Technologies*, 2015.
- [3] T.D. Ngo, A. Kashani, G. Imbalzano, K.T.Q. Nguyen, D. Hui, *Additive Manufacturing (3D printing): A review of materials, methods, applications and challenges*. *Compos. Part B Eng.* 143 (2018) 172–196.
- [4] P. Rochus, J.-Y. Plessier, M. Van Elsen, J.-P. Kruth, R. Carrus, T. Dormal, *New applications of rapid prototyping and rapid manufacturing (RP/RM) technologies for space instrumentation*. *Acta Astronaut.* 61 (2007) 352–359.
- [5] C.L. Ventola, *Medical Applications for 3D Printing: Current and Projected Uses*. *P T* 39 (2014) 704–11.
- [6] I. (Ian) Gibson, D.W. (David W.) Rosen, B. (Brent) Stucker, *Additive Manufacturing Technologies : Rapid Prototyping to Direct Digital Manufacturing*, Springer, 2010.
- [7] P.F. Egan, V.C. Gonella, M. Engensperger, S.J. Ferguson, K. Shea, *Computationally designed lattices with tuned properties for tissue engineering using 3D printing*. *PLoS One* 12 (2017) 1–21.
- [8] I. Buj-Corral, A. Bagheri, O. Petit-Rojo, *3D Printing of Porous Scaffolds with Controlled Porosity and Pore Size Values*. *Materials (Basel)*. 11 (2018) 1532.
- [9] D. Ahn, J.-H. Kweon, S. Kwon, J. Song, S. Lee, *Representation of surface roughness in fused-deposition modeling*. *J. Mater. Process. Technol.* 209 (2009) 5593–5600.
- [10] D. Ding, Z. Pan, D. Cuiuri, H. Li, S. Van Duin, N. Larkin, *Bead modelling and implementation of adaptive MAT path in wire and arc additive manufacturing*. *Robot. Comput. Integr. Manuf.* (2016).
- [11] I. Buj-Corral, O. Petit-Rojo, A. Bagheri, J. Minguella-Canela, *Modelling of porosity of 3D printed ceramic prostheses with grid structure*. *Procedia Manuf.* 13 (2017).
- [12] G. Hodgson, A. Ranelluci, J. Moe, *Slic3r Manual - Flow Math*, 2016.